JAERI-M
9509

ENERGY CONFINEMENT OF OHMICALLY HEATED D-SHAPED PLASMA IN DOUBLET III

(Doublet-III Experimental Report, 8)

May 1981

M. NAGAMI, H. YOKOMIZO, M. SHIMADA
H. YOSHIDA, K. IOKI,[*1] S. IZUMI,[*2] K. SHINYA[*3]
G. JAHNS,[*4] D. BAKER,[*4] C. ARMENTROUT[*4]
F. BLAU,[*4] E. FAIRBANKS,[*4] N. FUJISAWA
S. KONOSHIMA, S. SEKI, M.MAENO, AND
A. KITSUNEZAKI

日本原子力研究所
Japan Atomic Energy Research Institute

JAERI-M 9509

Energy Confinement of Ohmically Heated D-shaped Plasma in Doublet III (Doublet-III Experimental Report,8)

Masayuki NAGAMI, Hideaki YOKOMIZO, Michiya SHIMADA, Hidetoshi YOSHIDA
Kimihiro IOKI[*1], Shigeru IZUMI[*2], Kichiro SHINYA[*3], G. JAHNS[*4]
D. BAKER[*4], C. ARMENTROUT[*4], F. BLAU[*4], E. FAIRBANKS[*4],
Noboru FUJISAWA, Shigeru KONOSHIMA, Shogo SEKI, Masaki MAENO and
Akio KITSUNEZAKI

Division of Large Tokamak Development, Tokai Research Establishment, JAERI

(Received May 8, 1981)

Energy confinement properties were compared for D-shaped and circular cross section plasmas with an identical horizontal minor radius as functions of plasma current, electron density, and vertical elongation under a wide range of discharge conditions. The improvement of the energy confinement time with vertical elongation can be explained with an electron energy transport determined by $\bar{n}_e q^*$ and approximately neoclassical ion energy transport, both include the geometrical effect of vertical elongation. Particularly high current operation capability of D-shaped plasma produces remarkable improvement of energy confinement at high density region due to the reduction of neoclassical heat loss of ions. The highest energy confinement time (75 msec) is realized for a high current and high density D-shaped discharge.

Keywords; Doublet-III, D-shaped Cross Section, Energy Confinement, Neo-classical Theory, Joule Heating,

---

This work was performed under a cooperative agreement between the Japan Atomic Energy Research Institute and the United States Department of Energy under DOE Contract No. DE-AT03-80SF11512.

*1 On leave from Mitsubishi Atomic Power Industries.
*2 On leave from Hitachi, Ltd.
*3 On leave from Toshiba Corp.
*4 General Atomic Company, San Diego, California, U.S.A.

Doublet－Ⅲにおけるジュール加熱D形プラズマのエネルギ閉じ込め
（ダブレットⅢ実験報告・8）

日本原子力研究所東海研究所大型トカマク開発部
永見　正幸・横溝　英明・嶋田　道也・吉田　英俊
伊尾木公裕[*1]・出海　滋[*2]・新谷　吉郎[*3]
G. Jahns[*4]・D. Baker[*4]・C. Armentrout[*4]
F. Blau[*4]・E. Fairbanks[*4]・藤沢　登
木島　滋・関　省吾・前野　勝樹・狐崎　晶雄

（１９８１年５月８日受理）

Doublet－Ⅲにおいて，D形断面と円形断面プラズマの比較を広範囲のパラメーター領域で行ない，D形断面プラズマのエネルギ閉じ込め特性に関し以下の結果を得た。

1）最大プラズマ電流は，非円形度を考慮した安全係数 q_a^* で決まる。最大プラズマ密度は，プラズマ断面内の平均電流密度の大きさに依存する。

2）電子エネルギ閉じ込め時間は $\bar{n}_e q^*$ に比例し，イオンエネルギ閉じ込め時間は新古典理論の２倍までの大きさで説明される。特に，D形断面プラズマは円形断面プラズマに比較し大きなプラズマ電流を流せるため，高電子密度領域では，イオンのエネルギ損失を軽減することにより，エネルギ閉じ込め時間は著しく増大する。即ち，Doublet－Ⅲにおいて，エネルギ閉じ込め時間は，D形断面，大プラズマ電流，高電子密度条件下で最大（７５msec）となる。

＊1）外来研究員；三菱原子力工業（株）
＊2）外来研究員；日立製作所（株）
＊3）外来研究員；東京芝浦電気（株）
＊4）General Atomic Company

Contents

目　　次

1. INTRODUCTION

It is widely accepted that D-shaped cross section is one of the best for the application of future tokamak reactors because the D-shape is theoretically predicted to be the most stable under high β conditions.

Some characteristics of D-shaped or elliptic cross section plasmas have been reported by relatively small devices [1-3]. References [1-3] reported MHD properties and Ref. [1] reported observation of improvement of energy confinement time with vertical elongation of the plasma cross section.

This work will present energy confinement characteristics of ohmically heated D-shaped plasmas with the relatively large size of R ≃ 141 cm, a ≅ 44 cm, produced in the upper half of Doublet III.

The emphasis will be on the comparison of 1) operational regimes of plasma current and density, and 2) energy confinement, for D-shaped and circular cross section plasmas with an identical horizontal minor radius. Section 2 discusses the experimental procedure and evaluation of energy confinement; Section 3, the characteristics of the operational regime of D-shaped plasmas; Section 4, energy confinement properties; and the conclusions are discussed in Section 5.

2. EXPERIMENTAL PROCEDURE

Figure 1 shows a cross section view of Doublet III. The Doublet III tokamak [4] has the following parameters: major radius R ≅ 141 cm, plasma width 2a ≅ 90 cm, and toroidal field B_T = 24 kG. The Inconel 625 vacuum vessel is surrounded by 24 field shaping coils. Feedback control of the

1. INTRODUCTION

It is widely accepted that D-shaped cross section is one of the best for the application of future tokamak reactors because the D-shape is theoretically predicted to be the most stable under high β conditions.

Some characteristics of D-shaped or elliptic cross section plasmas have been reported by relatively small devices [1-3]. References [1-3] reported MHD properties and Ref. [1] reported observation of improvement of energy confinement time with vertical elongation of the plasma cross section.

This work will present energy confinement characteristics of ohmically heated D-shaped plasmas with the relatively large size of $R \simeq 141$ cm, $a \cong 44$ cm, produced in the upper half of Doublet III.

The emphasis will be on the comparison of 1) operational regimes of plasma current and density, and 2) energy confinement, for D-shaped and circular cross section plasmas with an identical horizontal minor radius. Section 2 discusses the experimental procedure and evaluation of energy confinement; Section 3, the characteristics of the operational regime of D-shaped plasmas; Section 4, energy confinement properties; and the conclusions are discussed in Section 5.

2. EXPERIMENTAL PROCEDURE

Figure 1 shows a cross section view of Doublet III. The Doublet III tokamak [4] has the following parameters: major radius $R \cong 141$ cm, plasma width $2a \cong 90$ cm, and toroidal field $B_T = 24$ kG. The Inconel 625 vacuum vessel is surrounded by 24 field shaping coils. Feedback control of the

magnetic flux linking the shaping coils allows the shape and position of many types of discharge to be controlled.

Plasma diagnostics used for the present study are:

1. Plasma equilibrium: 24 single turn flux loops to measure the distribution of the poloidal flux surface on the 24 shaping coils, and 12 magnetic probes. With the help of an MHD equilibrium code [5] the flux surface in the plasma is calculated. The resultant equilibrium is compared with the sawtooth observation by 10-channel and 19 channel horizontal and vertical soft X-ray diode arrays. The comparison shows good agreement.
2. Density distribution $n_e(r)$: 5-channel horizontal, tangential CO_2 laser interferometers.
3. Electron temperature distribution $T_e(r)$: electron cyclotron emission at the second harmonic, scanning soft X-ray energy spectrometer.
4. Ion temperature $T_i(o)$: charge exchange energy analyzer.
5. Radiative power loss: 5-channel bolometer array.
6. MHD activity: soft X-ray diode array.

The typical plasma equilibria used for this study are shown in Fig. 2; 1) K(a) = 1, K(o) = 1.0; 2) K(a) = 1.4, K(o) = 1.1; 3) K(a) = 1.7, K(o) = 1.3. As can be seen from these figures, magnetic surface within $r < 2/3a$ can be approximated with ellipses. The flux surface is approximated as an elliptic magnetic surface described by

$$K(r) = K(o) + [K(a) - K(o)](\frac{r}{a})^{\alpha} ,$$

for the evaluation of energy confinement, where K(r), K(o), K(a) are vertical elongation distributions as functions of plasma horizontal minor radius, vertical elongation at the plasma center and at the outermost magnetic surface.

For these equilibria $\alpha = 2$ produces good agreement with the results of the equilibrium calculation.

In the non-circular discharges, the plasma centers are shifted downward 9 - 14 cm from the horizontal observation of $n_e(r)$, $T_e(r)$ and $T_i(o)$. Therefore, for the convenience of the analysis, the measured $n_e(r)$, $T_e(r)$ are projected on the central horizontal plane along each magnetic surface.

The confinement properties are evaluated as follows:

$$\tau_{E_{eG}}(r) \equiv \int \frac{3}{2} n_e T_e dV \Big/ \int P_{oH} dV$$

$$\tau_{E_e}(r) \equiv \int \frac{3}{2} n_e T_e dV \Big/ \int P_{oH} - P_r - P_{ei} dV$$

$$\tau_{E_i}(r) \equiv \int \frac{3}{2} n_i T_i dV \Big/ \int P_{ei} dV$$

$$\tau_{E(r)} \equiv \int \frac{3}{2} (n_e T_e + n_i T_i) dV \Big/ \int P_{oH} \, dV$$

$$V(r) \equiv 2\pi R \, \pi K(r) \, r^2$$

where P_{oH} is the ohmic dissipation as determined from $P_{oH} = Vj/2\pi R$ (j = plasma current density), P_{ei} is the heat transfer from electrons to ions,

and P_r is the radiative power loss. The distribution of plasma current density is calculated using the Spitzer resistivity with trapped particle correction.

In the present energy confinement study, discharges are produced with a long flat top in plasma current and density of more than 300 to 400 msec to eliminate the ambiguity in calculating the energy confinement time caused by the inductive part of the loop voltage measurement and plasma energy change with time.

The plasma parameter regime used in this energy confinement study is shown in Table 1.

3. OPERATIONAL REGIME OF D-SHAPED PLASMAS

The maximum operational plasma current of D-shaped plasmas in Doublet III has been discussed in Ref. [6]. Similar results are reported in Ref. [1-3]. In those devices, the plasma current is limited at identical q_a^* for circular and elongated plasmas, where

$$q_a^* = \frac{2\pi a^2 B_T}{\mu_o IR} \frac{1 + K(a)^2}{2} \quad .$$

In Doublet III, q_a^* was limited around 2.5 - 2.7 before starting titanium gettering, and around 2.0 -2.5 after titanium gettering during Inconel is used as the material of primary limiter. After installing a TiC coated POCO-graphite limiter as the primary limiter (1980, summer), operation regime of q_a^* as low as 1.4 becomes possible in conjunction with Ti gettering. This paper will discuss the discharges with $q_a^* \gtrsim 2.4$. The properties of low q_a^* regime will be reported elsewhere.

and P_r is the radiative power loss. The distribution of plasma current density is calculated using the Spitzer resistivity with trapped particle correction.

In the present energy confinement study, discharges are produced with a long flat top in plasma current and density of more than 300 to 400 msec to eliminate the ambiguity in calculating the energy confinement time caused by the inductive part of the loop voltage measurement and plasma energy change with time.

The plasma parameter regime used in this energy confinement study is shown in Table 1.

3. OPERATIONAL REGIME OF D-SHAPED PLASMAS

The maximum operational plasma current of D-shaped plasmas in Doublet III has been discussed in Ref. [6]. Similar results are reported in Ref. [1-3]. In those devices, the plasma current is limited at identical q_a^* for circular and elongated plasmas, where

$$q_a^* = \frac{2\pi a^2 B_T}{\mu_o IR} \frac{1 + K(a)^2}{2} \quad .$$

In Doublet III, q_a^* was limited around 2.5 - 2.7 before starting titanium gettering, and around 2.0 -2.5 after titanium gettering during Inconel is used as the material of primary limiter. After installing a TiC coated POCO-graphite limiter as the primary limiter (1980, summer), operation regime of q_a^* as low as 1.4 becomes possible in conjunction with Ti gettering. This paper will discuss the discharges with $q_a^* \gtrsim 2.4$. The properties of low q_a^* regime will be reported elsewhere.

The maximum operational plasma density of D-shaped plasmas is also of practical importance. Figure 3 shows the comparison of maximum operational plasma density in circular and D-shaped plasmas under a same vacuum condition. The figure shows the relation of the averaged density $\bar{n}_e$ at the flat top of the discharge (from 500 ms to 800 ms) versus gas puff throughput Q between 300 msec and 500 msec in the discharges for K(a) = 1.0, K(a) = 1.4 with I_p = 350 kA and 530 kA at B_T = 24 kG.

In the comparison of the same I_p (350 kA) and different K, the density of circular discharges linearly increase with the increase of Q. With higher gas puffing than 55 Torr ℓ/sec the discharge becomes disruptive; therefore, the operational plasma density is limited at 5×10^{13} cm^{-3}. On the other hand, for K = 1.4 discharges, $\bar{n}_e$ saturates at 3.3×10^{13} cm^{-3}. This saturation is associated with a strong increase of particle recycling (H_α emission) at the plasma outer edge. It is necessary to operate K(a) = 1.4 D-plasmas at the same value of q_a^* (I_p = 530 kA) in order to obtain the same maximum plasma density achieved in circular plasmas with I_p = 350 kA. This dependence of maximum density on I_p is also observed for K = 1.0 plasmas: $\bar{n}_{e_{max}}$ increases from 5.0 to 6.4×10^{13} cm^{-3} by changing I_p from 350 kA to 530 kA, which is discussed in Ref. [7]. Therefore, for noncircular plasmas, $\bar{n}_{e_{max}}$ is determined by q_a^* for the same B_T. In other words, $\bar{n}_{e_{max}}$ is determined by average input power density or average current density $\bar{j}$, because for a similar q_a^*, $\bar{j}$ is proportional to $(1 + K^2)/2K$, which has little dependence on K.

4. ENERGY CONFINEMENT

The electron density profiles, measured with 5-channel CO_2 laser interferometers, are usually flat: between $1-(r/a)^4$ to $1-(r/a)^2$, and close to the former. In the calculation of plasma current density distribution versus minor radius, we assumed a constant Z_{eff}. This assumption produces good agreement with observations of sawtooth activity in the soft X-ray emission for respective discharges. It also is consistent with the Z_{eff} profile determined by the soft X-ray diode array and scanning soft X-ray energy spectrometer measurement except for low density operation, which shows a strong accumulation of metallic impurities [8]. Comparison of typical discharges of K(a) = 1.4 and K(a) = 1.0 at B_T = 24 kG, q_a^* = 4.6, $\bar{n}_e$ = 3.8 to 4.2 $\times 10^{13}$ cm^{-3} is shown in Fig. 4. The figure shows the profiles of T_e, q^*, P_{oH}, P_r and $\tau_{E_{eG}}$ as a function of horizontal minor radius. Although the plasma current and the total ohmic input power are different about 50%, the quantities shown in this figure are similar for circular and D-shaped plasmas of identical q_a^*. The T_e profile (therefore also the q^* profile) near the plasma center for D-shaped plasma is flatter than that for circular plasma with same q_a^*, but is similar to those with same I_p of 530 kA. The figure shows that ohmic input and energy transport is dominant at $r \lesssim a/2$ and radiative loss is dominat at $r \gtrsim a/2$. Therefore, we will discuss the energy transport property at $r \lesssim a/2$.

A result of the confinement analysis for a hydrogen discharge of B_T = 24 kG, I_p = 350 kA, K(a) = 1.0 is shown in Fig. 5 as a reference discharge (relatively small plasma current). The figure shows $\tau_{E_{eG}}$, $\langle 1 - P_r/P_{oH} \rangle$, τ_{E_e} and τ_{E_i} at $r \lesssim a/2$ as a function of line-averaged electron density $\bar{n}_e$, where $\langle 1 - P_r/P_{oH} \rangle = \int (1 - P_r/P_{oH})\, dV$ at $r \lesssim a/2$.

The ion temperature was not measured in this particular series. However, the charge exchange measurements in similar discharges of another series shows $T_i(o) \sim (0.75 - 1.0) \times T_e(o)$ for $\bar{n}_e$ = 2 to 6 $\times 10^{13}$ cm^{-3}. The calculation of $T_i(o)$ solving a one dimensional heat diffusion of ions on the basis of neoclassical heat transport, classical energy exchange between electrons and ions and charge exchange energy loss of ions shows that (1 to 2) × neoclassical heat transport of ions is consistent with the measurement within its experimental accuracy.

It is very difficult to distinguish the difference between 1 times and 2 times neoclassical transport of ions experimentally because the difference expected from the theory is less than 50 to 80 eV. Therefore calculation results for both cases are referred to here. The figure shows almost a flat dependence of $\tau_{E_{eG}}$ on $\bar{n}_e$, which is attributed to a continuous increment of loop voltage (from 1.15 V to 1.53 V) and to a reduction of the electron temperature with rising the electron density.

Under the condition of $T_e \cong T_i$, τ_{EeG} is expressed as

$$\tau_{E_{eG}} \cong \frac{\tau_E}{2} = \left\langle 1 - \frac{P_r}{P_{oH}} \right\rangle \frac{\tau_{E_e}\, \tau_{E_i}}{\tau_{E_e} + \tau_{E_i}} \quad .$$

Although $\langle P_r/P_{oH} \rangle$ increases slightly at the low and high density region, $\langle 1 - P_r/P_{oH} \rangle$ shows roughly a flat dependence on $\bar{n}_e$. Therefore, the flat dependence of $\tau_{E_{eG}}$ on $\bar{n}_e$ is caused mainly by an electron energy transport and (1 -2) × neoclassical transport of ions. The electron transport time τ_{E_e}, shown in the figure, has an Alcator type dependence of τ_{E_e} [sec] = 0.83 n_e [$\times 10^{14}$ cm^{-3}] a^2 [m], in which the coefficient has a similar magnitude as the ISX-A result [9].

Therefore, for the low current discharge of 350 kA, the energy confinement is effected by increasing electron-ion coupling which surpasses the continuing improvement of electron energy confinement time with rising density. The same behavior was originally discovered and discussed in Refs. [9, 10].

The electron transport times τ_{E_e} as a function of $\langle n_e \rangle$ are compared for different K and I_p in Fig. 6:

1. K(a) = 1.0, I_p = 350 kA.
2. K(a) = 1.0, I_p = 530 kA.
3. K(a) = 1.4, I_p = 350 kA.
4. K(a) = 1.4, I_p = 530 kA.

where $\langle n_e \rangle$ is the volume-averaged electron density inside r = a/2.

In each series of discharge, τ_{E_e} shows a linear dependence on $\langle n_e \rangle$. The figure shows the following:

1. For constant I_p, τ_{E_e} increases with the increase of K.
2. For constant K, τ_{E_e} decreases with the increase of plasma current.
3. For different K, τ_{E_e} is similar in the same q_a^*.

In the calculation of P_{ei} for elongated plasmas, neoclassical heat transport of ions

$$\bar{q}_i \propto \frac{nq^{*2}\nu_i\rho_T^2}{K^2}\frac{dT_i}{dr} \qquad (1)$$

is used [11] to calculate the ion temperature, where $\bar{q}_i$ is the ion heat flux averaged on a magnetic surface, ν_i is the collision frequency, and ρ_T is the toroidal Larmor radius.

Taking into account the above properties, several scaling laws of electron transport times are examined. The following simple expression shows one of the best fits to the present experiments:

$$\tau_{E_e} \propto \langle n_e\rangle q^* \propto \langle n_e\rangle \frac{B_T}{I_p}\cdot\frac{1+K^2}{2}$$

Figure 7 shows the relation $\tau_{E_e}\langle I_p\rangle/\left(B_T\cdot\frac{1+K\,(a/2)^2}{2}\right)$ versus $\langle n_e\rangle$ in the wide range of plasma parameters shown in the figure, where 1.5 times neoclassical is used as the ion energy confinement. $\langle I_p\rangle$ is the plasma current inside r = a/2. K(a/2) are 1.0, 1.2, 1.4 for discharges with K(a) = 1.0, 1.4, 1.7, respectively.

Now we can expect an improvement of gross energy confinement time for elongated plasmas for constant q_a^* particularly in high density regime, where neoclassical heat loss of ions is effective, because τ_{E_i} is improved by K^2 as is shown in Eq. (1) while $\tau_{E_e}(\propto nq^*)$ is kept constant. To demonstrate this advantage, three different K(a) deuterium discharges at constant q_a^* (= 4.3 -4.9) is compared. Figure 8(a) shows the comparison of $\tau_{E_eG}(a/2)$ in three series of discharges:

1. K(a) = 1.0, I_p = 350 kA (reference discharge)

2. K(a) = 1.4, I_p = 520 kA

3. K(a) = 1.7, I_p = 650 kA

The figures shows the following: 1) in low $\bar{n}_e$ regime of $\bar{n}_e \lesssim 3 \times 10^{13}$ cm^{-3}, $\tau_{E_{eG}}$ is the same for discharges with different K(a), 2) in high $\bar{n}_e$ regime of $\bar{n}_e \gtrsim 4 \times 10^{13}$ cm^{-3}, $\tau_{E_{eG}}$ is improved with the increase of vertical elongation. At highest n_e, $\tau_{E_{eG}}$ is improved by 65% with the vertical elongation from K(a) = 1.0 to 1.7. Since $T_i \simeq T_e$ for high density regime, the figure shows that the maximum gross energy confinement time τ_E reaches 75 ms.

This behavior of $\tau_{E_{eG}}$ may be attributed to the coupling of τ_{E_e} discussed before and τ_{E_i} determined by neoclassical transport. To understand the effect of elongation on energy confinement caused by the coupling of τ_{E_e} and τ_{E_i}, a simplified transport model in which τ_{E_e} and τ_{E_i} have dependencies only on $\langle n_e \rangle$, $\langle I_p \rangle$, K(a/2) is tried:

$$\tau_{E_e} = \frac{n}{I} \frac{1 + K^2}{2} \quad (\propto n_e q^*) \tag{2}$$

$$\tau_{E_{i_{NC}}} = \frac{I^2}{\left(\frac{1 + K^2}{2}\right)^2} \cdot \frac{K^2}{n} \quad \propto \left(\frac{K^2}{q^{*2} n_e}\right) \tag{3}$$

where n and I are non-dimensional electron density and plasma current.

In this series of experiment, $\langle 1 - P_r/P_{oH} \rangle$ is roughly constant with

$$\langle 1 - P_r/P_{oH} \rangle = 0.7 \pm 0.14 \quad .$$

Furthermore, since $T_e \simeq T_i$

$$\tau_{E_{eG}} \simeq \langle 1 - P_r/P_{oH} \rangle \frac{\tau_{E_e} \tau_{E_i}}{\tau_{E_e} + \tau_{E_e}} \propto \frac{\tau_{E_e} \tau_{E_i}}{\tau_{E_e} + \tau_{E_i}} \quad .$$

Therefore, comparisons of $\tau_{E_{eG}}$, which is experimentally obtained, and $\tau_{E_e}\tau_{E_i}/(\tau_{E_e} + \tau_{E_e})$, determined by the present transport model, may make clear the elongation effect in the experiment.

Figure 8(b) shows the model calculation of $2\tau_{E_e} \tau_{E_i}/(\tau_{E_e} + \tau_{E_i})$. n = 1 corresponds to $\tau_{E_e} = \tau_{E_i} = 1.0$ for the K(a) = 1.0, I_p = 350 kA series (reference discharge). Each curve shows the model calculation taking the ratio of $\langle I_p \rangle$ with respect to the reference discharge:

1. K(a/2) = 1.0, I = 1.0 for the discharge of K(a) = 1.0, I_p = 350 kA.
2. K(a/2) = 1.2, I = 1.3 for the discharge of K(a) = 1.4, I_p = 520 kA.
3. K(a/2) = 1.4, I = 1.7 for the discharge of K(a) = 1.7, I_p = 650 kA.

The term $1 + K^2/2I$ in τ_{E_e} of Eq. (2) are 1.0, 0.94, 0.87 for discharges No. 1, 2, 3, respectively. The term $I^2K^2/(1 + K^2/2)^2$ in τ_{E_i} of Eq. (3) are 1.0, 1.63, 2.58 for discharges No. 1, 2, 3, respectively. The model provides the same magnitude of $2 \tau_{E_e} \tau_{E_i}/(\tau_{E_e} + \tau_{E_i})$ for three discharges in n < 0.5. On the other hand, by the vertical elongation from 1.0 to 1.7, the model provides the improvement in $2 \tau_{E_e} \tau_{E_i}/(\tau_{E_e} + \tau_{E_i})$ of 1.29, 1.59, 1.9 at n = 1.0, 1.5, 2.0, respectively.

The comparison of experimental results and model calculations shows good agreement, if we assume n = 1 in the model corresponds to $\bar{n}_e = 3 \sim 4 \times 10^{13}$ cm^{-3} in the experiment. Similar transport analysis as is shown in Fig. 5 shows that this correspondence is reasonable. Because the neoclassical ion energy confinement time for deutrium discharge is 0.7 times of that of hydrogen ($\tau_{E_i} \propto 1/\sqrt{m}$, m is the mass of ions), and also the analysis shows that τ_{E_e} of deutrium discharge is a same magnitude within 20% as that of hydrogen, the $\bar{n}_e$ corresponding $\tau_{E_e} = \tau_{E_i}$ in deutrium discharge is smaller than that of hydrogen.

It becomes clear that energy confinement time is improved with increasing the plasma current in conjunction with the increase of vertical elongation. If we increase the plasma current with keeping the elongation constant, the $\tau_{E_{eG}}$ shows different behaviors from that shown in Fig. 8. Figure 9(a) shows the comparison of discharges with three different plasma currents and same K(a) of 1.4; 1) I_p = 350 kA, 2) 520 kA, 3) 1 MA. With increasing the plasma current, $\tau_{E_{eG}}$ is improved in high density regime. On the other hand, $\tau_{E_{eG}}$ of low density regime, where the electron transport is effective, declined with increasing the plasma current. These behaviors are well explained by the model transport of 1) I = 1.0, K(a/2) = 1.2, 2) I = 1.3, K(a/2) = 1.2 3) I = 2.4, K(a/2) = 1.3 as is shown in Fig. 9(b). Note that in high current (low q^*) operation of 1 MA, the vertical elongation at r = a/2 increases from 1.2 to 1.3.

In the discharge of I_p = 1 MA, up to 2 times neoclassical heat loss of ions is negligible ($P_{ei}/P_{OH} < 0.13$ at $r \leq a/2$) even in high $\bar{n}_e$ regime.

As a result, the Alcator type dependence appears in whole of the electron density region.

5. CONCLUSIONS

The following results have been obtained in the comparison of confinement properties in ohmically heated D-shaped and circular cross section plasmas with an identical horizontal minor radii.

1. Maximum operational plasma current is determined by the same q_a^* for the same B_T. Maximum operational electron density is determined by average current density (approximate average ohmic input power or q_a^*) i.e., D-shaped plasmas need larger plasma currents than circular plasmas corresponding to the identical q_a^* for the same B_T.
2. Transport properties are well explained by $\tau_{E_e} \propto n_e q^*$ and $\tau_{E_i} \sim$ up to 2 times neoclassical. The improvement of energy confinement time observed for D-shaped plasmas is due to the favorable geometrical effect of vertical elongation on the above transport properties, i.e., 1) for constant I_p and B_T, τ_{E_e} is improaved by $(1 + K^2)/2$, and 2) for constant q^* and B_T, τ_{E_i} is improved by K^2.
3. High current operation capability of D-shaped plasmas produce remarkable improvement of energy confinement at high plasma density region due to the reduction of neoclassical heat loss of ions. The highest τ_E (75 ms) is realized for high current D-shaped discharges.

As a result, the Alcator type dependence appears in whole of the electron density region.

5. CONCLUSIONS

The following results have been obtained in the comparison of confinement properties in ohmically heated D-shaped and circular cross section plasmas with an identical horizontal minor radii.

1. Maximum operational plasma current is determined by the same q_a^* for the same B_T. Maximum operational electron density is determined by average current density (approximate average ohmic input power or q_a^*) i.e., D-shaped plasmas need larger plasma currents than circular plasmas corresponding to the identical q_a^* for the same B_T.
2. Transport properties are well explained by $\tau_{E_e} \propto n_e q^*$ and $\tau_{E_i} \sim$ up to 2 times neoclassical. The improvement of energy confinement time observed for D-shaped plasmas is due to the favorable geometrical effect of vertical elongation on the above transport properties, i.e., 1) for constant I_p and B_T, τ_{E_e} is improaved by $(1 + K^2)/2$, and 2) for constant q^* and B_T, τ_{E_i} is improved by K^2.
3. High current operation capability of D-shaped plasmas produce remarkable improvement of energy confinement at high plasma density region due to the reduction of neoclassical heat loss of ions. The highest τ_E (75 ms) is realized for high current D-shaped discharges.

ACKNOWLEDGEMENT

The continuing support of Drs. S. Mori, Y. Iso, K. Tomabechi, Y. Obata, M. Yoshikawa in JAERI, and Dr. T. Ohkawa in GAC is gratefully acknowledged. This experiment was carried out with the fine support of the diagnostics group under Dr. R. Fisher and the machine operation group under Dr. R. Callis. The authors would like to thanks Drs. R. Waltz and W. Pfeiffer for stimulating discussions on ion energy confinement.

This work was authorized by a cooperative agreement between Japan Atomic Energy Research Institute and the United States Department of Energy under DOE Contract No. DE-AT03-80ET51019.

REFERENCES

[1] FREEMAN, R. L., ADCOCK, S. J., BAUER, J. F., BROOKS, N. H., DeBOO, J. C., et al., (Proc. 7th Int. Conf. Innsbruck, 1976) Vol 1, IAEA, Vienna (1977) 317; FREEMAN, R. L., ADCOCK, S. J., BROOKS, N. H. DeBOO, J. C., FISHER, R. K., et al., A comparison of circular and elliptic plasmas in Doublet-IIA, GA-A13781.

[2] McGUIRE, K., ROBINSON, D. C., WOOTON, A. J., in Plasma Physics and Controlled Nuclear Fusion Research (Proc. 7th Int. Conf. Innsbruck, 1978) Vol. 1, IAEA, Vienna (1979) 387.

[3] TOYAMA, H., IWAHASHI, A., KANEKO, H., KAWADA, Y., MAKISHIMA, K., et al., ibid Vol. 1, IAEA, Vienna (1979) 365.

ACKNOWLEDGEMENT

The continuing support of Drs. S. Mori, Y. Iso, K. Tomabechi, Y. Obata, M. Yoshikawa in JAERI, and Dr. T. Ohkawa in GAC is gratefully acknowledged. This experiment was carried out with the fine support of the diagnostics group under Dr. R. Fisher and the machine operation group under Dr. R. Callis. The authors would like to thanks Drs. R. Waltz and W. Pfeiffer for stimulating discussions on ion energy confinement.

This work was authorized by a cooperative agreement between Japan Atomic Energy Research Institute and the United States Department of Energy under DOE Contract No. DE-AT03-80ET51019.

REFERENCES

[1] FREEMAN, R. L., ADCOCK, S. J., BAUER, J. F., BROOKS, N. H., DeBOO, J. C., et al., (Proc. 7th Int. Conf. Innsbruck, 1976) Vol 1, IAEA, Vienna (1977) 317; FREEMAN, R. L., ADCOCK, S. J., BROOKS, N. H. DeBOO, J. C., FISHER, R. K., et al., A comparison of circular and elliptic plasmas in Doublet-IIA, GA-A13781.

[2] McGUIRE, K., ROBINSON, D. C., WOOTON, A. J., in Plasma Physics and Controlled Nuclear Fusion Research (Proc. 7th Int. Conf. Innsbruck, 1978) Vol. 1, IAEA, Vienna (1979) 387.

[3] TOYAMA, H., IWAHASHI, A., KANEKO, H., KAWADA, Y., MAKISHIMA, K., et al., ibid Vol. 1, IAEA, Vienna (1979) 365.

[4] OHKAWA, T., in Controlled Fusion and Plasma Physics (9th Europ. Conf. Oxford, 1979), Vol. 2, invited papers, Culham Lab. (1979) 321.

[5] McCLAIN, F. W., BROWN, B. B., GAQ, A Computer Program to Find and Analyze Axisymmetric MHD Plasma Equilibria, GA-A14490 (1977).

[6] KITSUNEZAKI, A., et al., presented at 8th Int. Conf. on Cont. Nucl. Fus. Res. (1980) Brussels.
JAERI Team, Nucl. Fusion 20 (1980) 1455.

[7] EQUIPE TFR, Nucl. Fusion 20 (1980) 1227.

[8] FUJISAWA, N., NAGAMI, M., YOKOMIZO, H., SHIMADA, M., KONOSHIMA, S., et al., Impurity Status of D-Shaped Discharges in Doublet III with Inconel Wall and Limiters, JAERI-M 9181.

[9] MURAKAMI, M., NIELSON, G. H., HOWE, H. C., JERNIGAN, T. C., BATES, S. C., et al., Phys. Rev. Lett. 42 (1979) 655.

[10] WALTZ, R. E., GUEST, G. E., Phys. Rev. Lett. 42 (1979) 651.

[11] TSANG, K. T., The Physics of Fluids, 20 (1977) 1680.

TABLE 1
PLASMA PARAMETERS

R	141 cm
a	44 cm
K(a)	1.0 - 1.7
B_T	15 - 24 kG
I_p	250 kA - 1 MA
n_e	$1.3 - 6.7 \times 10^{13}$ cm^{-3}
$T_e(o)$	490 - 1240 eV
Z_{eff}	$\lesssim 1.6$
Working gas	H_2, D_2

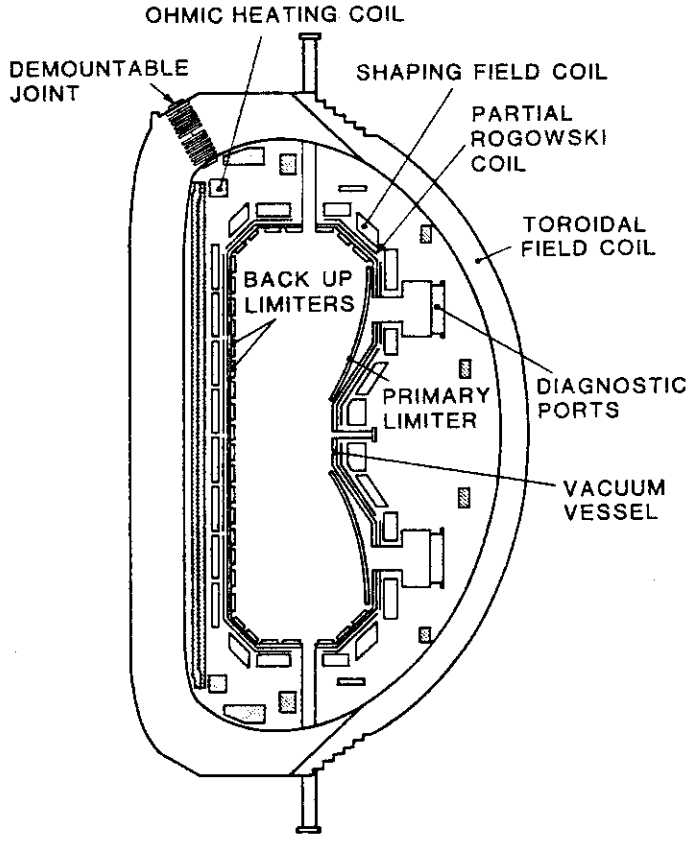

Fig.1 Cross sectional view of Doublet-III device

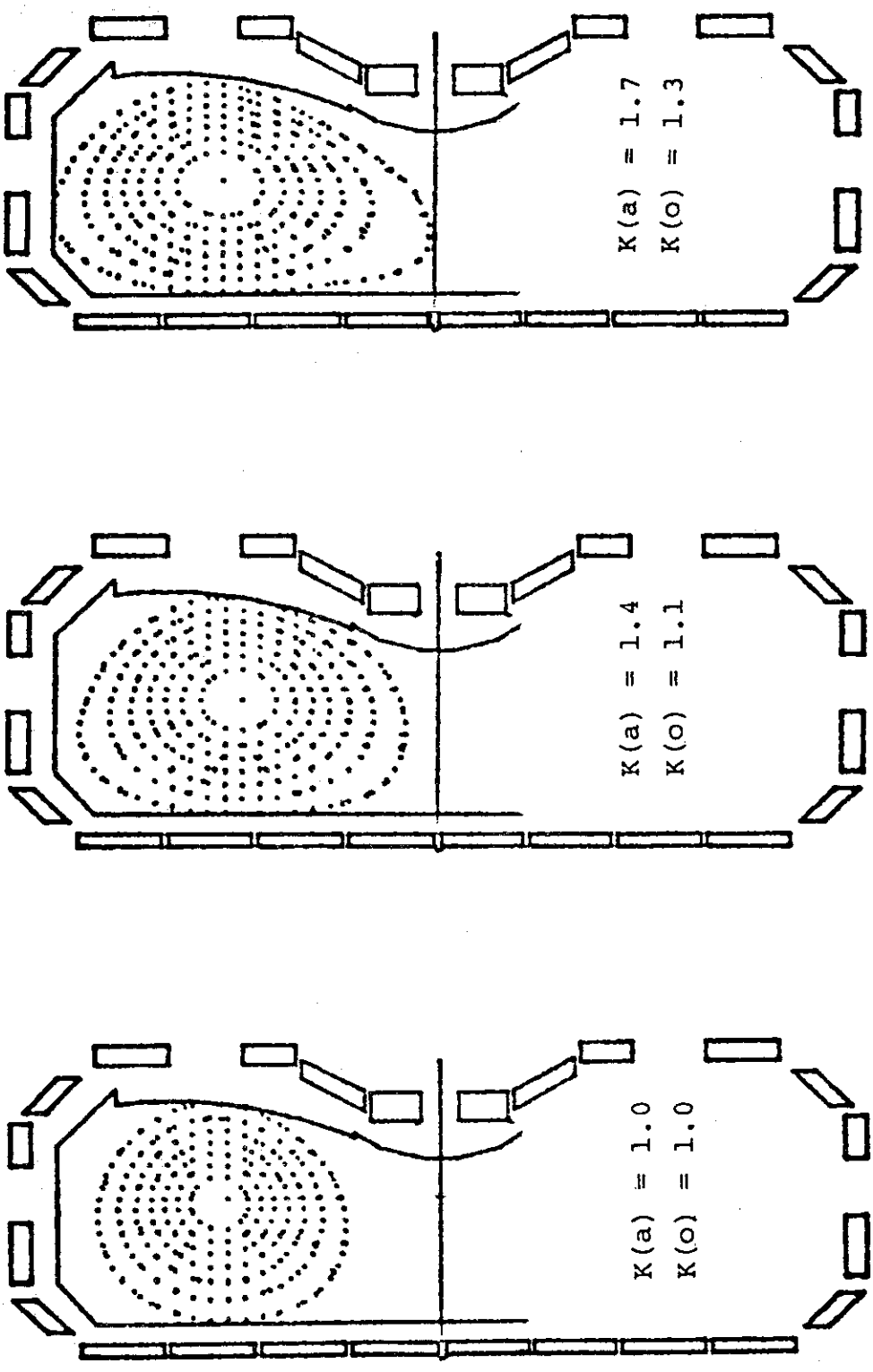

Fig.2 Three typical equilibria used in this study. K(a) and K(o) are the vertical elongation of magnetic surface at the plasma outer edge and plasma center, respectively

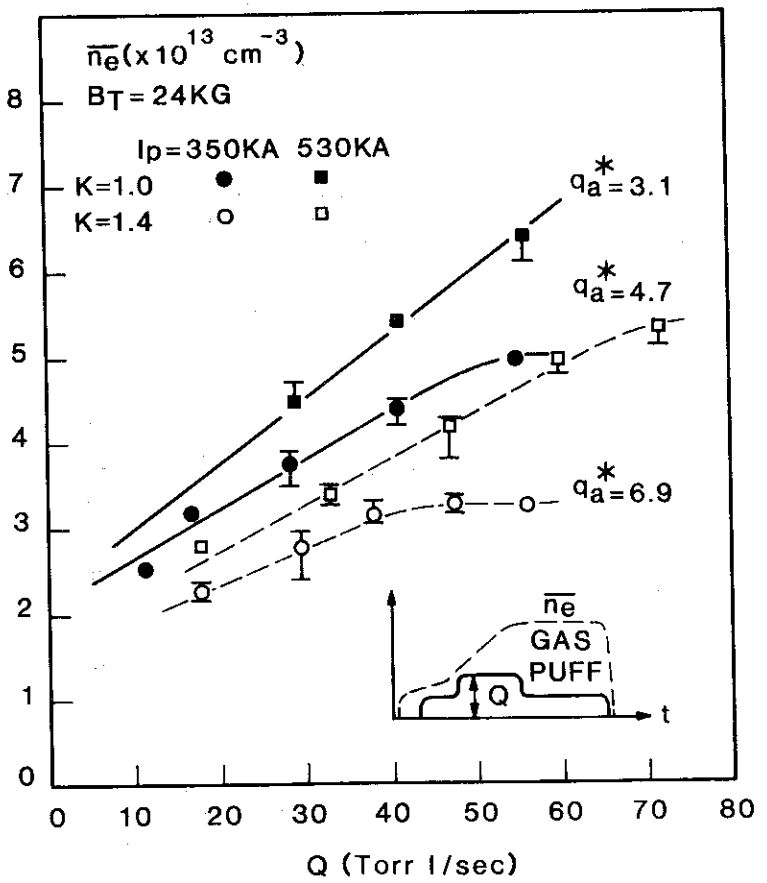

Fig.3 Line averaged electron density $\bar{n}_e$ at the flat top of the discharge versus gas puff throughput Q between 300 to 500 msec for four different series of discharge. In each series, discharge becomes disruptive when $\bar{n}_e$ is higher than maximum $\bar{n}_e$ shown here. It is necessary to operate D-plasmas at the same value of q_a^* in order to obtain the same maximum $\bar{n}_e$ achieved in circular plasma

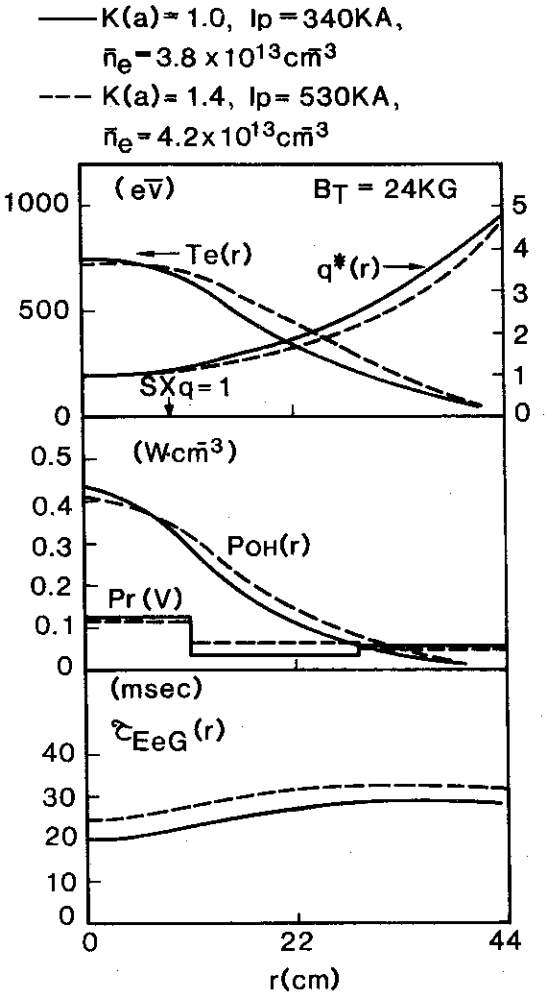

Fig.4 Comparison of D-shaped and circular cross section plasmas of same q_a^* and B_T; the electron temperature T_e, the safety factor q^*, the ohmic dissipation P_{OH}, the radiative power loss P(r), the gross electron energy confinement time $\tau_{E_{eG}}$

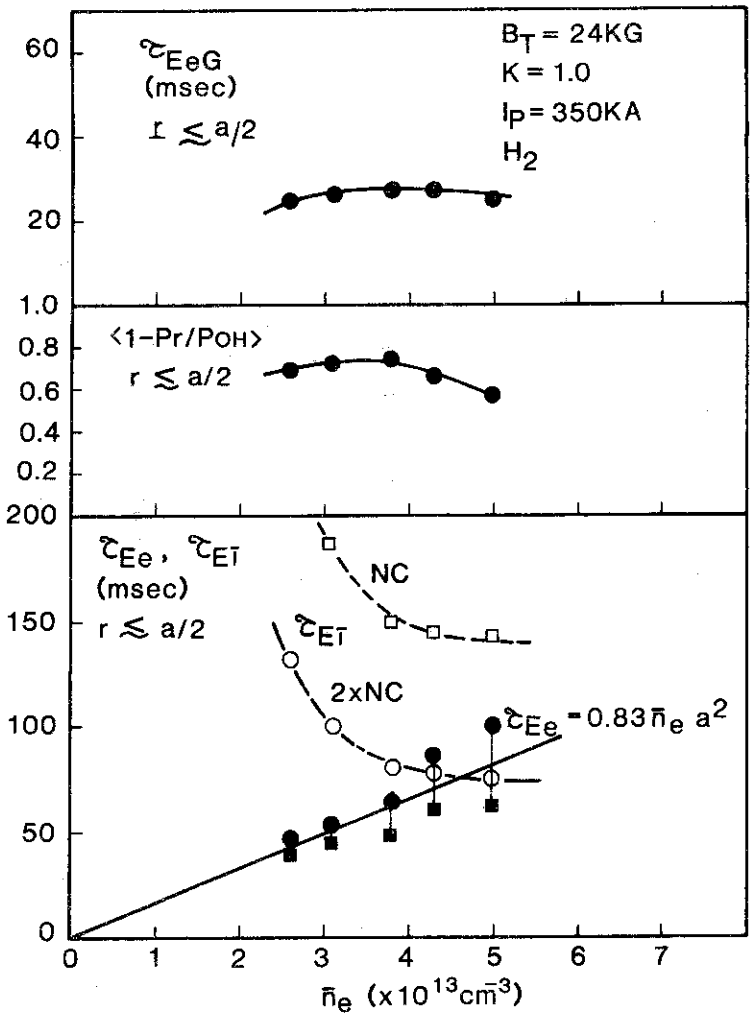

Fig.5 A result of energy confinement analysis for discharges with relatively small plasma current. The gross electron energy confinement time $\tau_{E_{eG}}$ shows flat dependence on $\bar{n}_e$. $\tau_{E_{eG}}$ is effected by increasing electron-ion coupling which surpasses the continuing improvement of the electron energy transport time τ_{E_e} with rising plasma density

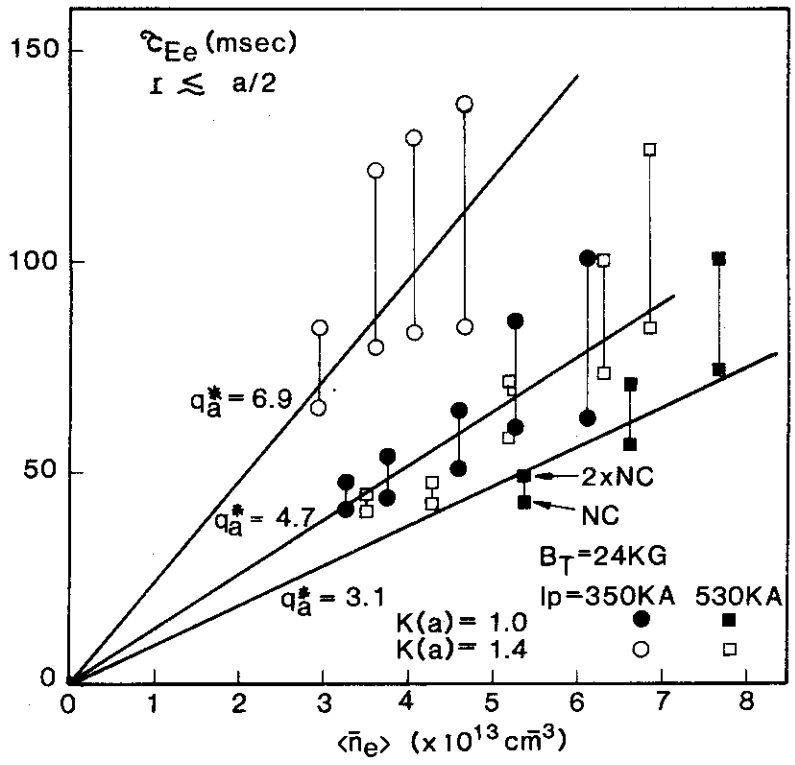

Fig.6 Comparisons of electron energy transport time τ_{E_e} for discharges with different I_p and K(a). For constant K(a), τ_{E_e} increases with the increase of K(a). For constant K(a), τ_{E_e} decreases with the increase of plasma current. τ_{E_e} is similar for same q_a^* and different K(a)

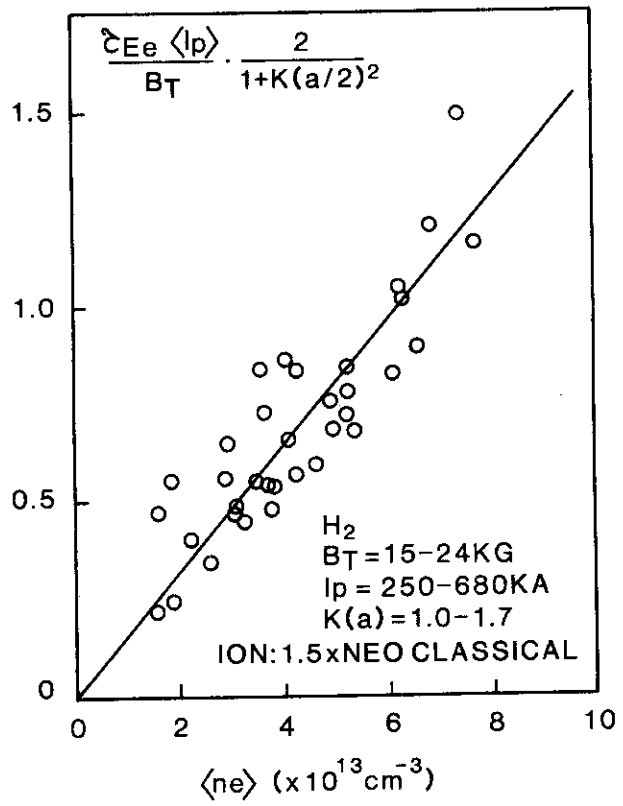

Fig.7 The relation $\tau_{E_e} \langle I_p \rangle / (B_T \cdot (1 + K(a/2)^2)/2)$ versus $\langle n_e \rangle$. τ_{E_e} is proportional to $\langle n_e \rangle$ q*

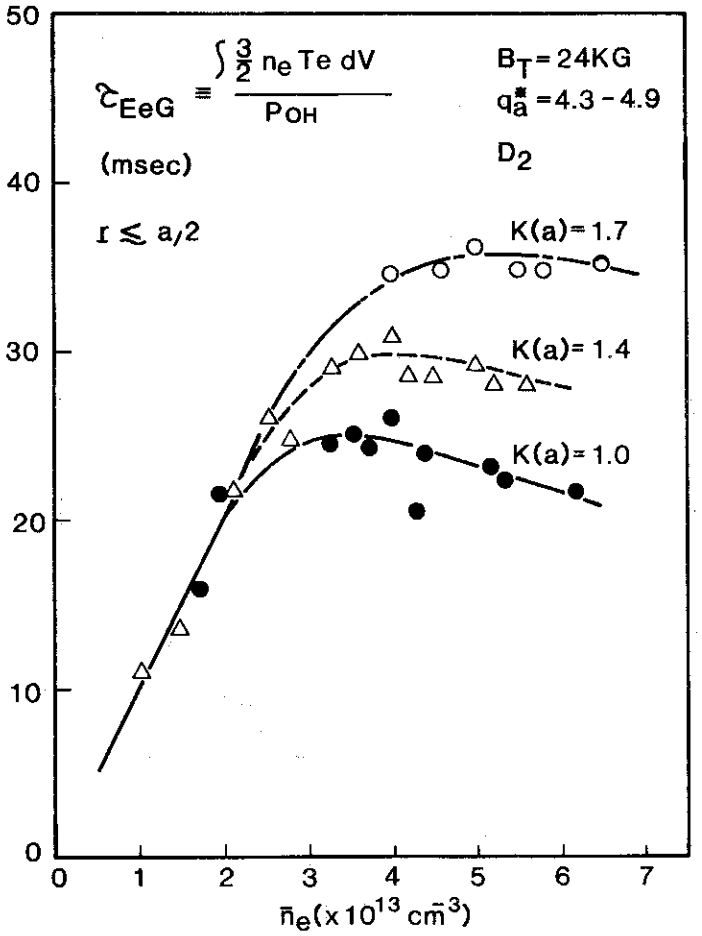

Fig.8(a) Comparison of $\tau_{E_{eG}}$ for discharges of K(a) = 1.0, 1.4 and 1.7 with constant q_a^*. At high density region, $\tau_{E_{eG}}$ is improved by 65% with the vertical elongation from K(a) = 1.0 to 1.7

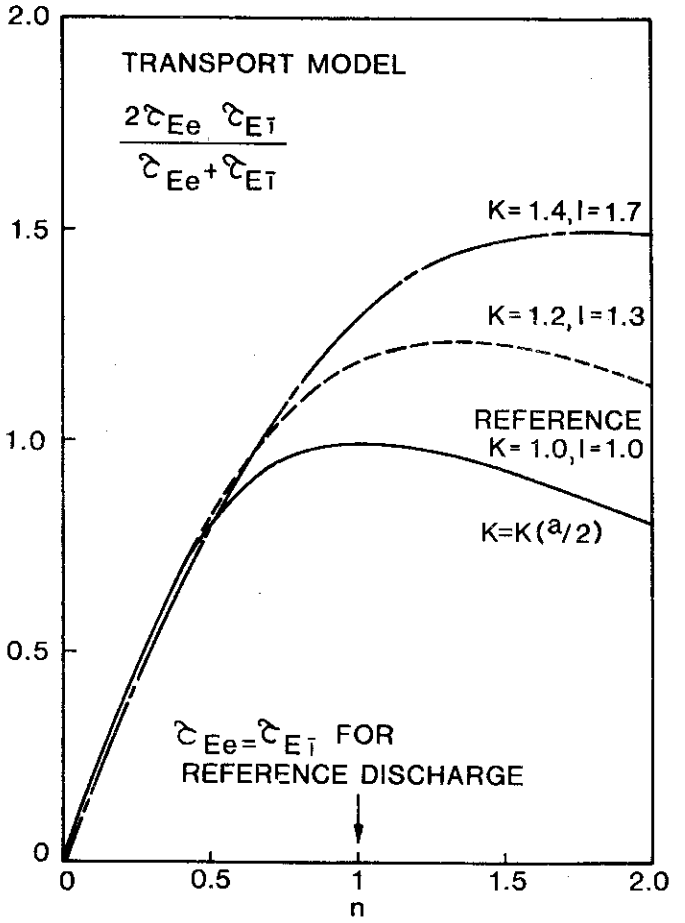

Fig.8(b) Transport model calculation based on equation (2) and (3). n and I are non-dimensional electron density and plasma current.

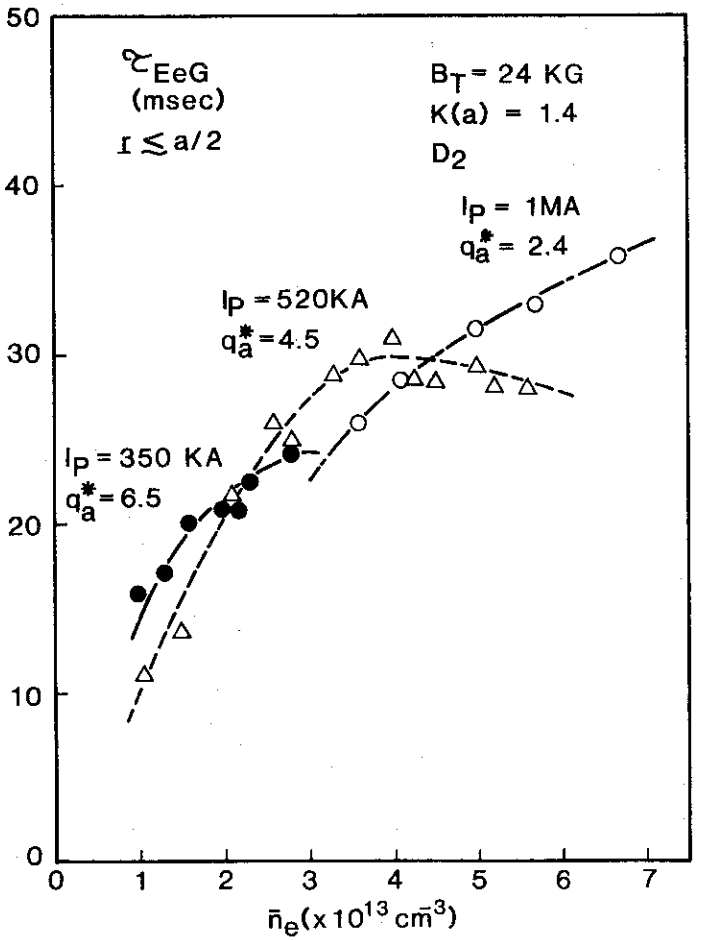

Fig.9(a) Comparison of $\tau_{E_{eG}}$ for descharges of I_p = 350 kA, 520 kA and 1 MA with constant K(a). 1 MA discharge shows roughly a linear dependence of $\tau_{E_{eG}}$ on $\bar{n}_e$ in whole region of $\bar{n}_e$

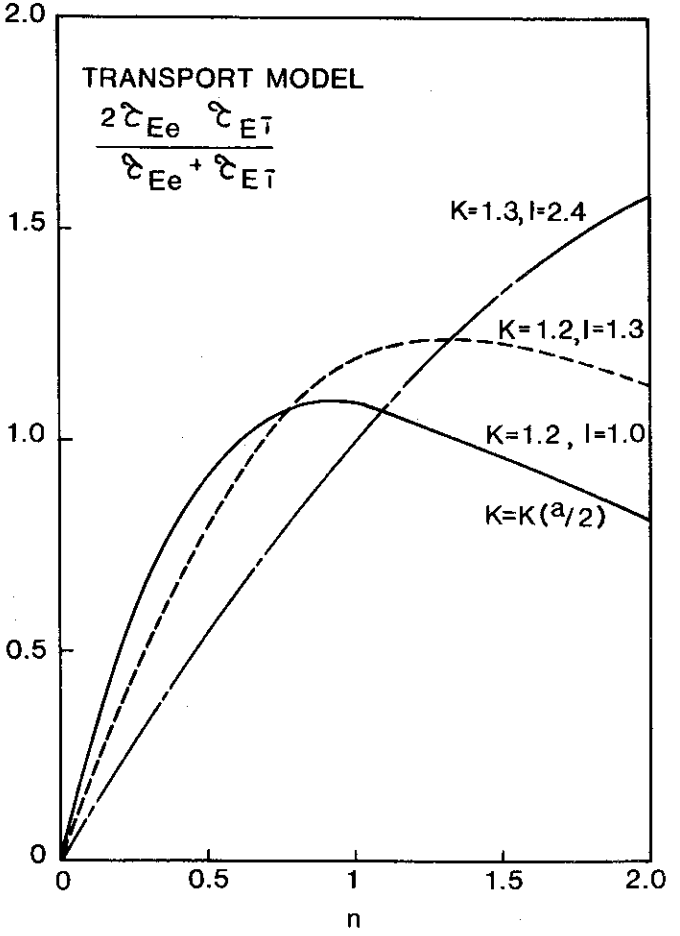

Fig.9(b) Transport model calculation based on equation (2) and (3)